

Article

# New Quinolone-Based Thiosemicarbazones Showing Activity Against *Plasmodium falciparum* and *Mycobacterium tuberculosis*

Richard M. Beteck <sup>1,\*</sup>, Ronnett Seldon <sup>2</sup>, Audrey Jordaan <sup>3</sup>, Digby F. Warner <sup>3,4,5</sup>, Heinrich C. Hoppe <sup>6,7</sup>, Dustin Laming <sup>7</sup> and Setshaba D. Khanye <sup>1,7,\*</sup>

<sup>1</sup> Division of Pharmaceutical Chemistry, Faculty of Pharmacy, Rhodes University, Grahamstown 6140, South Africa

<sup>2</sup> Drug Discovery and Development Centre (H3-D), Department of Chemistry, University of Cape Town, Rondebosch 7701, South Africa; ronnett.seldon@uct.ac.za

<sup>3</sup> SAMRC/NHLS/UCT Molecular Mycobacteriology Research Unit, Department of Pathology, University of Cape Town, Observatory 7925, South Africa; audrey.jordaan@uct.ac.za (A.J.); Digby.Warner@uct.ac.za (D.F.W.)

<sup>4</sup> Institute of Infectious Disease and Molecular Medicine, University of Cape Town, Observatory 7925, South Africa

<sup>5</sup> Wellcome Centre for Infectious Diseases Research in Africa, University of Cape Town, Observatory 7925, South Africa

<sup>6</sup> Department of Biochemistry and Microbiology, Faculty of Science, Rhodes University, Grahamstown 6140, South Africa; h.hoppe@ru.ac.za

<sup>7</sup> Centre for Chemo- and Biomedical Research, Rhodes University, Grahamstown 6140, South Africa; dustinlaming89@gmail.com

\* Correspondence: richmbi1@yahoo.com (R.M.B.); s.khanye@ru.ac.za (S.D.K.); Tel.: +27-46-603-8397 (S.D.K.)

Received: 9 March 2019; Accepted: 9 April 2019; Published: 4 May 2019



**Abstract:** Co-infection of malaria and tuberculosis, although not thoroughly investigated, has been noted. With the increasing prevalence of tuberculosis in the African region, wherein malaria is endemic, it is intuitive to suggest that the probability of co-infection with these diseases is likely to increase. To avoid the issue of drug-drug interactions when managing co-infections, it is imperative to investigate new molecules with dual activities against the causal agents of these diseases. To this effect, a small library of quinolone-thiosemicarbazones was synthesised and evaluated in vitro against *Plasmodium falciparum* and *Mycobacterium tuberculosis*, the causal agents of malaria and tuberculosis, respectively. The compounds were also evaluated against HeLa cells for overt cytotoxicity. Most compounds in this series exhibited activities against both organisms, with compound **10**, emerging as the hit; with an MIC<sub>90</sub> of 2 µM against H37Rv strain of *M. tuberculosis* and an IC<sub>50</sub> of 1 µM against the 3D7 strain of *P. falciparum*. This study highlights quinolone-thiosemicarbazones as a class of compounds that can be exploited further in search of novel, safe agents with potent activities against both the causal agents of malaria and tuberculosis.

**Keywords:** Co-infections; thiosemicarbazones; quinolones; malaria; *Mycobacterium tuberculosis*

## 1. Introduction

*Mycobacterium tuberculosis* (*Mtb*) is a pathogenic bacterium that causes tuberculosis, primarily a pulmonary infection in humans [1]. This bacterium currently infects about one-third of the world population [2]; however, a healthy immune system suppresses growth and multiplication of *Mtb* to an extent that the bacterium remains inactive and unable to cause pathology [3]. This is the case for 90% of people harbouring *Mtb* [4].

When the immune system becomes suppressed or weakened as is the case during treatment of rheumatoid arthritis, HIV infection, and old age, *Mtb* reactivates, and consequently latent tuberculosis is converted to active pulmonary tuberculosis [5]. Other factors promoting conversion to the active state include diabetes and malnutrition [6]. People with active pulmonary tuberculosis suffer from symptoms of the disease [7] and can infect others [8]. An estimated 10.0 million people worldwide were reported to be infected by active pulmonary tuberculosis, and 1.3 million people died as consequence in 2017 [9]. The disease is currently treated using a first line regiment of four drugs (rifampicin, isoniazid, pyrazinamide, ethambutol), which must be taken daily for at least six months [10]. The current management and/or treatment of tuberculosis is complicated, and the situation has been worsened by the emergence and spread of multi-drug resistant and extensively drug resistant forms of *Mtb* strains [11]. There is therefore a great need to research new chemical agents with the potential to inhibit *Mtb* infection.

On the other hand, malaria is currently the third leading cause of deaths from a single infective agent. It caused ill health in 216 million people, and reportedly led to the death of 445,000 people in 2016 [12]. The disease is the biggest burden to Sub-Saharan Africa, wherein 88% of malarial cases and 90% of the reported deaths occurred [13]. *Plasmodium falciparum* is one of the five *Plasmodium* species responsible for malaria infection in humans [14]. It is the most virulent of all species [15] and accounts for 90–99% of the global malaria cases [16]. Although the death toll due to malaria has witnessed a decline over the past fifteen years [17], malaria is still a great global health challenge, with at least 40% of the world's population currently living in places endemic to this disease [18] and 90 countries still having ongoing malaria transmission [16]. The current scenario of malaria is worrisome, and is characterised by the emergence and spread of parasites resistant to all current treatment options, including artemisinins, the current treatment gold standard [19,20]. Artemisinin combination therapy (ACTs) is the recommended treatment for uncomplicated malaria [21], while quinine or artesunate administered parenterally is recommended for the treatment of complicated malaria [22].

A great common trait between malaria and tuberculosis is the development of resistance. A careful look into the history of malarial chemotherapy and treatment of tuberculosis suggests that the pathogens responsible for these diseases have an inherent ability to develop resistance over any drug used against them, irrespective of whether the drug(s) is used in mono- or combination therapy [23,24]. It is noteworthy to emphasise that these two diseases share common endemicity and the issue of co-infection with both diseases has been reported [25]. With increasing prevalence of TB in the African region (the area with the highest malaria prevalence), there is likely to be a high prevalence of TB and malaria co-infection. Furthermore, it has been noted that malaria causes a deterioration in TB treatment outcome [25] and commonly deployed anti-malarials such as chloroquine and quinine are counter-indicative with fluoroquinolones, second line anti-TB agents [26]. Taking these in consideration, it should be intuitive to search for new molecules with the potential to act as anti-malarial and anti-TB agents.

Thioacetazone (**1**, Figure 1), a thiosemicarbazone-containing compound, is a potent anti-TB drug. Inherent toxicities issues associated with the use of this drug especially in situations of HIV infection, a common TB co-infection, has jeopardised further clinical deployment of this drug [27]. Other thiosemicarbazone containing compounds (**2**, Figure 1) have been reported to exhibit anti-malarial activity [28]. Fluoroquinolones (**3**, Figure 1), a sub-class of quinolones, are recommended second line therapy for TB [29]. More importantly, fluoroquinolones have also been reported for their anti-malarial potential (**4**, Figure 1) [30]. In recent work, we reported quinolones incorporating a hydrazide-hydrazone moiety (**5**, Figure 1), which exhibited potent activity against *Mtb* [31]. Considering these literatures precedents, we reasoned that design and development of novel compounds incorporating both thiosemicarbazone and quinolone frameworks might be worth exploiting as potential compounds to target both malaria and TB infections. Herein, we report the synthesis of heterocyclic compounds with thiosemicarbazone and quinolone motifs at their core structure. In vitro biological evaluations showcase these compounds as potent inhibitors of both *P. falciparum* and *M. tuberculosis*.

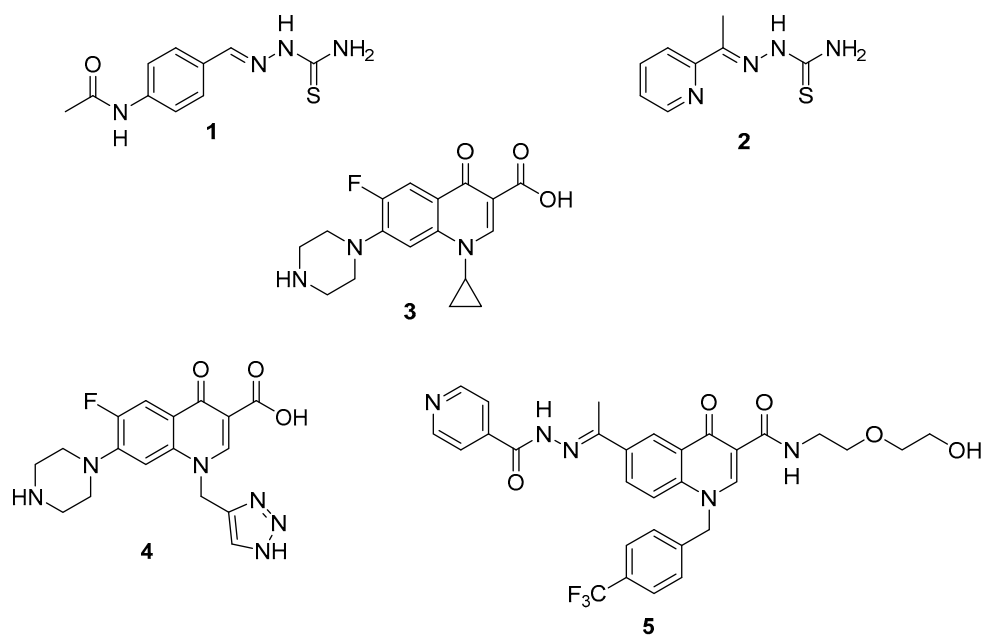
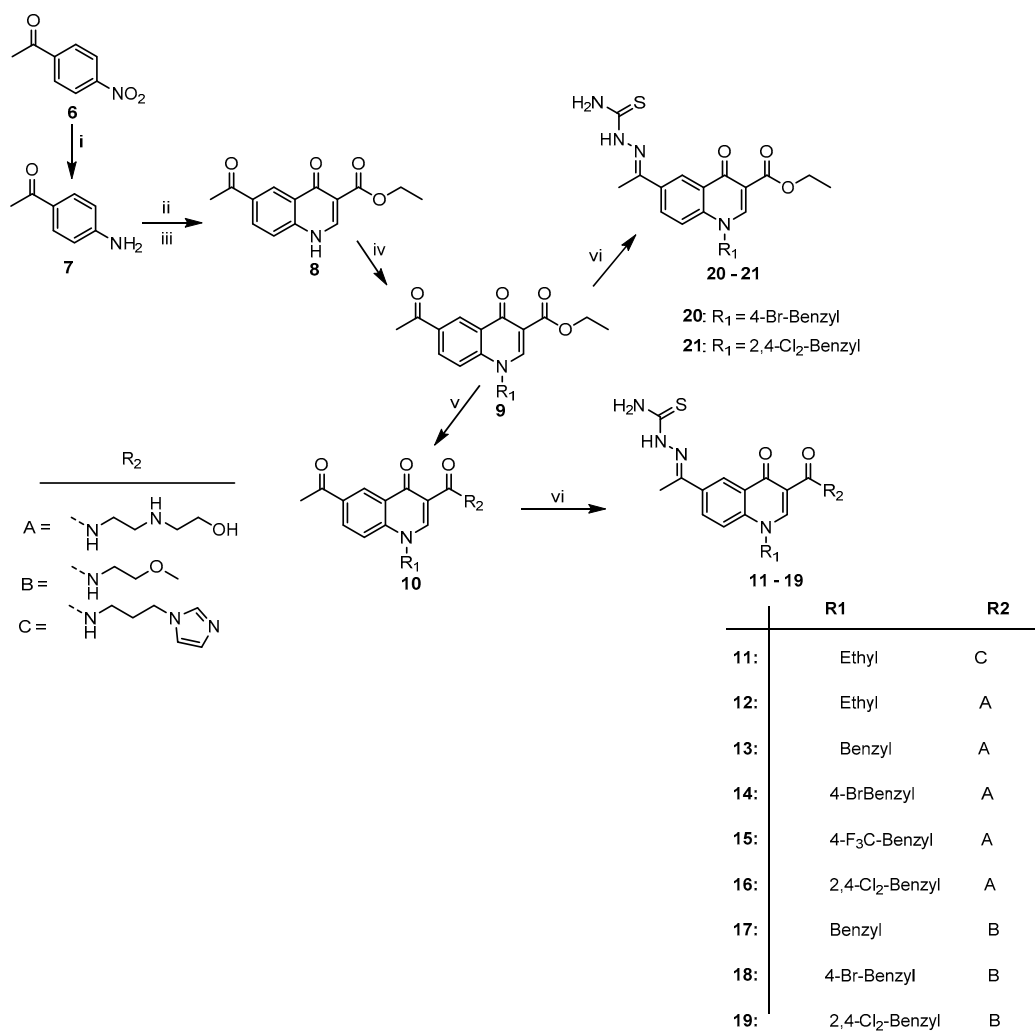


**Figure 1.** Thiosemicarbazones and quinolones exhibiting antimalarial and anti-TB activity.

## 2. Results and Discussion

### 2.1. Chemistry

Our target compounds were obtained following the synthetic routes presented in Scheme 1 below. Briefly, the reduction of *p*-nitroacetophenone **6** using reduced iron powder and ammonium chloride in refluxing ethanol afforded *p*-aminoacetophenone **7**. Compound **7** was condensed with diethyl ethoxy methylenemalonate, and following a classical Gould-Jacobs cyclization procedure for quinolone synthesis [32], later cyclised in boiling diphenylether to obtain intermediate **8** in 50–70% yields. Compound **8**, just like most quinolones reported in literature, is practically not soluble in any solvent [32]; this partly could be attributed to *pi-pi* stacking promoted by the highly planar nature of this fragment in particular, and the quinolone nucleus in general. It was therefore essential to modify this fragment in such a way as to disrupt planarity, and/or introduce hydrophilic moieties before appending a thiosemicarbazone unit, this was achieved through *N*-alkylation of the secondary amine and aminolysis of the ester functionalities in **8**. *N*-alkylation of the secondary amine was achieved following treatment with alkyl/aryl halides under refluxing DMF using  $K_2CO_3$  as a base to afford intermediate **9** in 50–70% yields. Compound **9** was subjected to aminolysis by treatment with hydrophilic amines in the presence of DBU under refluxing conditions to obtain **10** as amide derivative in 40% yield. Treatment of **9**, or **10** with equimolar amounts of thiosemicarbazide and a few drops of acetic acid gave target compounds **11–21** in 60–80% yields. The structures of target compounds were confirmed using  $^1H$  and  $^{13}C$  NMR, high resolution mass spectrometry analysis also confirmed the pseudomolecular ion peaks consistent with structures of achieved compounds. (See Supplementary Materials). The signal appearing at *ca* 10.11 ppm on the  $^1H$  NMR spectra of compound **11–19** is indicative of the presence of an amide proton ( $-CONH-$ ), this signal is absent in the  $^1H$  NMR spectra of compound **20** and **21**, both of which lack the corresponding amide. The peak at *ca* 10.37 ppm on the  $^1H$  NMR spectra of all target compounds is attributable to the hydrazinic proton ( $-C(=S)NH-N=$ ). The thioamide protons ( $-C(=S)NH_2$ ) could be observed at two different chemical shifts, *ca* 8.3 ppm and 8.00 ppm. These differences in chemical shift to protons attached to the same atom have been attributed to the lack of free rotation brought about by the formation of carbon-nitrogen double bond character around C-N bond of the thioamide [33].



**Scheme 1.** Synthesis of target compounds 11–21<sup>a</sup>. <sup>a</sup> Reagents and conditions: (i) Reduced Fe powder, NH<sub>4</sub>Cl; (ii) Acetonitrile, diethyl ethoxymethylenemalonate, reflux 12 h; (iii) Diphenyl ether, 250 °C, 5 min; (iv) K<sub>2</sub>CO<sub>3</sub>, DMF, alkyl/arylhalide (1.2–5 eqv), 7 h; (v) Amine (5 eqv), DBU (1.2 eqv), CHCl<sub>3</sub>, reflux 12 h; thiosemicarbazide, AcOH (cat), EtOH, reflux overnight.

## 2.2. Pharmacology

All target compounds were screened for in vitro inhibitory activity against the 3D7 strain of *P. falciparum* and the *M. tuberculosis* H37Rv strain. Target compounds were also evaluated in vitro against human cervix adenocarcinoma (HeLa) cell for overt cytotoxicity. Emetine, a cytotoxic agent, was used as a reference in the latter assay. At 20 μM, none of the compounds suppressed HeLa cell viability below 80%, suggesting that they pose little cytotoxicity risk at this concentration. Target compounds were evaluated for their potential to inhibit the growth of *M. tuberculosis* in vitro using middlebrook 7H9 media supplemented with casitone, glucose and tylopol [34]. The H37Rv strain of *Mtb* was deployed in this study, and rifampicin was used as a reference. The anti-*Mtb* activity of compounds in this study is reported as the minimum inhibitory concentration required to inhibit 90% (MIC<sub>90</sub>) of the bacteria population and the data is summarised in Table 1 below. Except compound 11, all compounds were active against *Mtb*; exhibiting activity in the range of 2–100 μM.

The anti-*Mtb* potential of this series appeared to be strongly influenced by the nature of substituents at position -1 and -3 of the quinolone ring. For-example, comparing compound 20 (MIC<sub>90</sub>; 102.5 μM) with compound 14 (MIC<sub>90</sub>; 10.3 μM) indicates that an amide at position -3 promotes activity over an ester group. This observation is also evident when comparing compound 21 (MIC<sub>90</sub>; 31.6 μM) with compound 16 (MIC<sub>90</sub>; 4.8 μM). Structure-activity relationship analysis further suggests that activity

increases with increasing hydrophilicity of the amide moiety at position -3. This is observed when comparing the structure and activity of, for example, compound **17** (MIC<sub>90</sub>; 44.2 μM) with compound **13** (MIC<sub>90</sub>; 2.7 μM), compound **11** (MIC<sub>90</sub>; >125 μM) versus compound **12** (MIC<sub>90</sub>; 73.4 μM). Moreover, comparing the structure and activity of compound **13** (MIC<sub>90</sub>; 2.7 μM) with compound **12** (MIC<sub>90</sub>; 73.4 μM) highlights that the presence of benzyl unit at position -1 seems to be favoured over an alkyl chain. There, is however, lack of a clear correlation of how the substitution pattern on the benzyl unit influences activity.

**Table 1.** In vitro antiplasmodial and antimycobacterial activities of quinolone-based thiosemicarbazones.

Compound	MIC <sub>90</sub> (μM)		ClogP <sup>a</sup>
	H37Rv	Pf 3D7	
<b>11</b>	>125	3.7	−0.02
<b>12</b>	73.4	na	−1.17
<b>13</b>	2.7	4.1	0.18
<b>14</b>	10.3	4.7	0.95
<b>15</b>	2.0	1.2	0.75
<b>16</b>	4.8	3.1	1.38
<b>17</b>	44.2	24.6	1.07
<b>18</b>	15.0	9.9	1.84
<b>19</b>	10.2	na	2.27
<b>20</b>	102.5	na	2.55
<b>21</b>	31.6	na	3.52
<b>CQ</b>	-	0.012	-
<b>RF</b>	0.062	-	-

<sup>a</sup> Calculated using ACD/ChemSketch freeware version 12.0, na = not active, RF = Rifampicin, CQ = Chloroquine.

To investigate anti-plasmodial activity, target compounds were screened in vitro against the chloroquine sensitive strain (3D7) of *P. falciparum* in a pLDH assay using chloroquine as the reference. Activity of these compounds together with the reference compound is reported as IC<sub>50</sub>, concentration required to inhibit 50% parasite growth and is incorporated in Table 1. Most compounds in this series exhibited activity in the low micromolar range (IC<sub>50</sub> less than 5 μM). The anti-plasmodial activity of this series follows the same pattern noted for anti-*Mtb* activity. For example, comparing compound **12** (not active against 3D7) and **8** (IC<sub>50</sub>; 4 μM), both of which differ only on the nature of substituent at position -1, suggest that a benzyl unit at this position leads to favourable anti-plasmodial activity. Compound **20**, bearing an ethyl ester at position -3, is devoid of activity, while compound **14**, its amide derivative, exhibited an IC<sub>50</sub> value of 4 μM. This observation points to the fact that an amide at this position greatly enhances activity over an ester moiety.

### 3. Materials and Methods

#### 3.1. General Information

Chemicals and solvents deployed in this study were purchased from various chemical vendors: Sigma-Aldrich (Pty) Ltd. (Johannesburg, South Africa), Merck (Pty) Ltd. (Johannesburg, South Africa) and were used as purchased. The progress of the reactions was monitored by thin layer chromatography (TLC) using Merck 60F254 silica gel plates (Merck, Johannesburg, South Africa) supported on aluminum and the plates were visualized under ultraviolet (UV 254 and 366 nm) light and in iodine flasks. Where necessary, the crude compounds were purified by means of a silica gel column chromatography using Merck Kieselgel 60 Å: 70–230 (0.068–0.2 mm) silica gel mesh (Merck, Johannesburg, South Africa). <sup>1</sup>H and <sup>13</sup>C NMR spectra were recorded on Bruker Biospin 300 MHz spectrometer, and the chemical shifts (δ) are given in values referenced to deuterated DMSO-*d*<sub>6</sub> and are reported in parts per million (ppm). Proton chemical shifts for deuterated DMSO appear at 2.5 ppm for <sup>1</sup>H and 39.5 ppm for <sup>13</sup>C-NMR.

Proton coupling patterns are abbreviated as follows: s (singlet), d (doublet), t (triplet), q (quartet), and m (multiplet). Coupling constant ( $J$ ) are reported in Hz. The high-resolution mass spectrometric data (HRS-MS) of final compounds were recorded on Waters Synapt G2 Mass Spectrometer (Stellenbosch University, South Africa) using electrospray ionization (ESI) in the positive ionization mode. Melting points were obtained using a Reichert hot stage microscope and are reported as obtained. The starting compounds 7–10 were synthesized from the commercial accessible *p*-nitroacetophenone 6 as previously described in the literature [34]. Purity was determined by HPLC (Agilent, Santa Clara, CA, USA), and all compounds were confirmed to have purity >95% using a similar method previously described [35].

### 3.2. General Synthetic Procedure for the Quinolone-Thiosemicarbazone Derivatives, 11–21

In a round bottom flask containing 400 mg of compound 9 or 10 dissolved in 95% ethanol (20 mL) was added 1.2 equivalence of thiosemicarbazide followed by a few drops of glacial acetic acid. The reaction mixture was stirred under reflux overnight, left to cool to room temperature. The formed precipitates were filtered, washed with  $2 \times 10$  mL ice cold ethanol and air dried to obtain target compounds, 11–21, in 60–80% yields.

(*E*)-*N*-(3-(1*H*-imidazol-1-yl)propyl)-6-(1-(2-carbamothioylhydrazono)ethyl)-1-ethyl-4-oxo-1,4-dihydroquinolone-3-carboxamide, **11**. Brown powder. Yield = 80% (0.35 g). m.p.: 187–189 °C.  $^1\text{H-NMR}$  (300 MHz, DMSO- $d_6$ )  $\delta_{\text{H}}$  (ppm): 10.37 (s, 1H, CSNHN), 10.04 (t,  $J = 5.8$  Hz, 1H, CONH), 8.86 (s, 1H, Ar-H), 8.69–8.47 (m, 3H, Ar-H), 8.36 (s, 1H, NH), 8.03 (s, 1H, NH), 7.83 (d,  $J = 9.2$  Hz, 1H, Ar-H), 7.68 (s, 1H, Ar-H), 7.22 (s, 1H, Ar-H), 4.53 (q,  $J = 6.9$  Hz, 2H,  $-\text{CH}_2\text{CH}_3$ ), 4.03 (t,  $J = 6.9$  Hz, 2H,  $-\text{CH}_2-$ ), 3.60–3.29 (m, 6H,  $2 \times -\text{CH}_2$ , overlap with  $d\text{H}_2\text{O}$ ), 2.40 (s, 3H,  $\text{CH}_3$ ), 1.39 (t,  $J = 6.9$  Hz, 3H,  $-\text{CH}_2\text{CH}_3$ ).  $^{13}\text{C-NMR}$  (75 MHz, DMSO- $d_6$ )  $\delta_{\text{C}}$  (ppm): 179.9, 173.1, 165.4, 148.1, 146.4, 140.0, 137.4, 134.6, 131.4, 128.3, 126.9, 124.7, 120.1, 117.9, 111.9, 56.3, 48.2, 44.6, 35.5, 15.2, 14.2.  $m/z$  (ESI-MS) found 440.1860, calcd for  $\text{C}_{21}\text{H}_{26}\text{N}_7\text{O}_2\text{S}$  440.1869  $[\text{M} + \text{H}]^+$ . HPLC purity > 96%,  $rt = 8.2$  min.

(*E*)-6-(1-(2-carbamothioylhydrazono)ethyl)-1-ethyl-*N*-(2-((2-hydroxyethyl)amino)ethyl)-4-oxo-1,4-dihydroquinolone-3-carboxamide, **12**. Yellow powder. Yield = 60% (0.2 g). m.p.: 183–185 °C.  $^1\text{H-NMR}$  (300 MHz, DMSO- $d_6$ )  $\delta_{\text{H}}$  (ppm): 10.35 (s, 1H, CSNHN), 10.12 (t,  $J = 4.9$  Hz, 1H, CONH), 8.86 (s, 1H, Ar-H), 8.69–8.47 (m, 2H, Ar-H), 8.36 (s, 1H, NH), 8.03 (s, 1H, NH), 7.83 (d,  $J = 8.9$  Hz, 1H, Ar-H), 5.31 (s, 1H, OH), 4.53 (q,  $J = 6.8$  Hz, 2H,  $-\text{CH}_2\text{CH}_3$ ), 3.74–3.54 (m, 5H,  $-\text{NH}-$ ,  $2 \times -\text{CH}_2-$ ), 3.21–2.95 (m, 4H,  $2 \times -\text{CH}_2-$ ), 2.39 (s, 3H,  $\text{CH}_3$ ), 1.43 (t,  $J = 6.8$  Hz, 3H,  $-\text{CH}_2\text{CH}_3$ ).  $^{13}\text{C-NMR}$  (75 MHz, DMSO- $d_6$ )  $\delta_{\text{C}}$  (ppm): 179.4, 175.4, 165.9, 148.7, 146.8, 140.0, 135.1, 131.9, 127.9, 124.7, 117.9, 111.6, 56.8, 49.5, 49.1, 46.9, 35.9, 15.1, 14.2.  $m/z$  (ESI-MS) found 419.1971, calcd for  $\text{C}_{19}\text{H}_{27}\text{N}_6\text{O}_3\text{S}$  419.1966  $[\text{M} + \text{H}]^+$ . HPLC purity > 96%,  $rt = 6.4$  min.

(*E*)-1-benzyl-6-(1-(2-carbamothioylhydrazono)ethyl)-*N*-(2-((2-hydroxyethyl)amino)ethyl)-4-oxo-1,4-dihydroquinolone-3-carboxamide, **13**. White powder. Yield = 70% (0.34 g). m.p.: 197–199 °C.  $^1\text{H-NMR}$  (300 MHz, DMSO- $d_6$ )  $\delta_{\text{H}}$  (ppm): 10.35 (s, 1H, CSNHN), 10.10 (t,  $J = 5.6$  Hz, 1H, CONH), 9.08 (s, 1H, Ar-H), 8.64–8.44 (m, 2H, Ar-H), 8.32 (s, 1H, NH), 8.02 (s, 1H, NH), 7.67 (d,  $J = 9.2$  Hz, 1H, Ar-H), 7.47–7.10 (m, 5H, Ar-H), 5.83 (s, 2H,  $-\text{CH}_2\text{Ar}$ ), 5.30 (s, 1H, OH), 3.94–3.51 (m, 5H,  $-\text{NH}-$ ,  $2 \times -\text{CH}_2-$ ), 3.16 (t,  $J = 5.6$  Hz, 2H,  $-\text{CH}_2-$ ), 3.05 (t,  $J = 6.7$  Hz, 2H,  $-\text{CH}_2-$ ), 2.36 (s, 3H,  $-\text{CH}_3$ ).  $^{13}\text{C-NMR}$  (75 MHz, DMSO- $d_6$ )  $\delta_{\text{C}}$  (ppm): 179.9, 175.8, 165.9, 149.1, 146.4, 139.9, 136.8, 135.5, 131.4, 129.6, 129.2, 128.3, 127.9, 127.4, 126.9, 124.22, 119.2, 111.9, 56.8, 56.3, 49.9, 46.8, 35.9, 14.2.  $m/z$  (ESI-MS) found 481.1930, calcd for  $\text{C}_{24}\text{H}_{29}\text{N}_6\text{O}_3\text{S}$  481.1925  $[\text{M} + \text{H}]^+$ . HPLC purity > 96%,  $rt = 8.5$  min.

(*E*)-1-(4-bromobenzyl)-6-(1-(2-carbamothioylhydrazono)ethyl)-*N*-(2-((2-hydroxyethyl)amino)ethyl)-4-oxo-1,4-dihydroquinolone-3-carboxamide, **14**. White powder. Yield = 80% (0.34 g). m.p.: 200–202 °C.  $^1\text{H-NMR}$  (300 MHz, DMSO- $d_6$ )  $\delta_{\text{H}}$  (ppm): 10.36 (s, 1H, CSNHN), 10.11 (t,  $J = 5.8$  Hz, 1H, CONH), 9.08 (s, 1H, Ar-H), 8.61–8.44 (m, 2H, Ar-H), 8.33 (s, 1H, NH), 8.01 (s, 1H, NH), 7.64 (d,  $J = 9.8$  Hz, 1H, Ar-H), 7.55 (d,  $J = 8.4$  Hz, 2H, Ar-H), 7.19 (d,  $J = 8.4$  Hz, 2H, Ar-H), 5.82 (s, 2H,  $-\text{CH}_2\text{Ar}$ ), 5.27 (s, 1H, OH), 3.77–3.63 (m, 5H,  $-\text{NH}-$ ,  $2 \times -\text{CH}_2-$ ), 3.16 (t,  $J = 6.1$  Hz, 2H,  $-\text{CH}_2-$ ), 3.09–3.00 (m, 2H,  $-\text{CH}_2-$ ), 2.36 (s, 3H,  $-\text{CH}_3$ ).  $^{13}\text{C-NMR}$  (75 MHz, DMSO- $d_6$ )  $\delta_{\text{C}}$  (ppm): 179.5, 175.4, 165.4, 146.4, 144.1, 140.0, 136.4, 135.1,

134.6, 132.4, 129.6, 127.9, 124.2, 121.9, 118.3, 111.9, 56.3, 55.4, 50.0, 47.2, 35.9, 14.2.  $m/z$  (ESI-MS) found 559.1123, calcd for  $C_{24}H_{28}BrN_6O_3S$  559.1127  $[M + H]^+$ . HPLC purity > 96%,  $rt = 9.4$  min.

(*E*)-6-(1-(2-carbamothioylhydrazono)ethyl)-*N*-(2-((2-hydroxyethyl)amino)ethyl)-4-oxo-1-(4-(trifluoromethyl)benzyl)-1,4-dihydroquinolone-3-carboxamide, **15**. White powder. Yield = 80% (0.35 g). m.p.: 199–201 °C.  $^1H$ -NMR (300 MHz, DMSO- $d_6$ )  $\delta_H$  (ppm): 10.37 (s, 1H, CSNHN), 10.11 (s, 1H, CONH), 9.12 (s, 1H, Ar-H), 8.56 (s, 1H, Ar-H), 8.32 (s, 1H, CSNH), 8.01 (s, 1H, CSNH), 7.87 – 7.27 (m, 6H, Ar-H), 5.97 (s, 2H,  $-CH_2Ar$ ), 5.26 (s, 1H, OH), 3.79 – 3.50 (m, 4H,  $2 \times -CH_2$ ), 3.10 – 2.87 (m, 5H,  $-NH$ ,  $2 \times -CH_2$ ), 2.36 (s, 3H,  $-CH_3$ ).  $^{13}C$ -NMR (75 MHz, DMSO- $d_6$ )  $\delta_C$  (ppm): 179.9, 175.8, 165.9, 149.6, 146.4, 141.4, 140.5, 135.5, 135.0, 131.7, 127.6, 127.5, 126.3, 124.7, 122.9, 118.3, 112.5, 56.8, 55.4, 49.5, 47.3, 35.9, 14.2.  $m/z$  (ESI-MS) found 549.1790, calcd for  $C_{25}H_{28}F_3N_6O_3S$  549.0896  $[M + H]^+$ . HPLC purity > 96%,  $rt = 9.4$  min.

(*E*)-6-(1-(2-carbamothioylhydrazono)ethyl)-1-(2,4-dichlorobenzyl)-*N*-(2-((2-hydroxyethyl)amino)ethyl)-4-oxo-1,4-dihydroquinolone-3-carboxamide, **16**. Off white powder. Yield = 80% (0.32 g). m.p.: 205–207 °C.  $^1H$ -NMR (300 MHz, DMSO- $d_6$ )  $\delta_H$  (ppm): 10.39 (s, 1H, CSNHN), 10.10 (t,  $J = 5.0$  Hz, 1H, CONH), 9.12 (s, 1H, Ar-H), 8.69 – 8.47 (m, 2H, Ar-H), 8.36 (s, 1H, CSNH), 8.05 (s, 1H, CSNH), 7.78 – 7.50 (m, 3H, Ar-H), 7.15 (dd,  $J = 7.8, 5.8$  Hz, 1H, Ar-H), 5.85 (s, 2H,  $-CH_2Ar$ ), 5.32 (t,  $J = 4.7$  Hz, 1H, OH), 3.92 – 3.54 (m, 5H,  $-NH$ ,  $2 \times -CH_2$ ), 3.16 (t,  $J = 5.9$  Hz, 2H,  $-CH_2$ ), 3.05 (t,  $J = 5.0$  Hz, 2H,  $-CH_2$ ), 2.36 (s, 3H,  $-CH_3$ ).  $^{13}C$ -NMR (75 MHz, DMSO- $d_6$ )  $\delta_C$  (ppm): 179.4, 176.3, 165.4, 149.9, 146.4, 145.9, 139.6, 137.7, 135.5, 132.4, 131.9, 131.4, 131.0, 129.6, 127.4, 124.7, 118.8, 111.9, 57.2, 55.4, 49.5, 46.8, 35.9, 14.2.  $m/z$  (ESI-MS) found 549.1126, calcd for  $C_{24}H_{27}Cl_2N_6O_3S$  549.1119  $[M + H]^+$ . HPLC purity > 96%,  $rt = 9.1$  min.

(*E*)-1-benzyl-6-(1-(2-carbamothioylhydrazono)ethyl)-*N*-(2-methoxyethyl)-4-oxo-1,4-dihydroquinolone-3-carboxamide, **17**. Off white powder. Yield = 73% (0.34 g). m.p.: 199–200 °C.  $^1H$ -NMR (300 MHz, DMSO- $d_6$ )  $\delta_H$  (ppm): 10.43 (s, 1H, CSNHN), 10.17 (t,  $J = 5.0$  Hz, 1H, CONH), 9.14 (s, 1H, Ar-H), 8.70 – 8.50 (m, 2H, Ar-H), 8.40 (s, 1H, NH), 8.11 (s, 1H, NH), 7.73 (d,  $J = 8.7$  Hz, 1H, Ar-H), 7.48 – 7.16 (m, 5H, Ar-H), 5.88 (s, 2H,  $-CH_2Ar$ ), 3.66 – 3.52 (m, 4H,  $2 \times -CH_2$ ), 3.37 (s, 3H, OCH<sub>3</sub>), 2.42 (s, 3H, CH<sub>3</sub>).  $^{13}C$ -NMR (75 MHz, DMSO- $d_6$ )  $\delta_C$  (ppm): 179.9, 175.8, 164.4, 146.8, 140.5, 136.8, 134.6, 131.9, 130.1, 129.6, 129.2, 128.3, 127.9, 127.4, 126.9, 125.1, 118.3, 111.6, 71.7, 58.5, 57.2, 38.7, 14.2.  $m/z$  (ESI-MS) found 452.1660, calcd for  $C_{23}H_{26}N_5O_3S$  452.0981  $[M + H]^+$ . HPLC purity > 96%,  $rt = 9$  min.

(*E*)-1-(4-bromobenzyl)-6-(1-(2-carbamothioylhydrazono)ethyl)-*N*-(2-methoxyethyl)-4-oxo-1,4-dihydroquinolone-3-carboxamide, **18**. Brown powder. Yield = 60% (0.25 g). m.p.: 204–206 °C.  $^1H$ -NMR (300 MHz, DMSO- $d_6$ )  $\delta_H$  (ppm): 10.34 (s, 1H, CSNHN), 10.07 (t,  $J = 5.1$  Hz, 1H, CONH), 9.09 (s, 1H, Ar-H), 8.64 – 8.47 (m, 2H, Ar-H), 8.31 (s, 1H, NH), 8.02 (s, 1H, NH), 7.64 – 7.44 (m, 3H, Ar-H), 7.20 (d,  $J = 8.9$  Hz, 2H, Ar-H), 5.80 (s, 2H,  $-CH_2Ar$ ), 3.60 – 3.46 (m, 4H,  $2 \times -CH_2$ ), 3.26 (s, 3H, OCH<sub>3</sub>), 2.36 (s, 3H, CH<sub>3</sub>).  $^{13}C$ -NMR (75 MHz, DMSO- $d_6$ )  $\delta_C$  (ppm): 180.4, 175.8, 164.5, 149.6, 146.4, 139.6, 136.5, 135.1, 132.4, 131.5, 129.2, 127.4, 124.7, 121.5, 118.8, 111.9, 71.3, 58.5, 55.9, 38.7, 13.8.  $m/z$  (ESI-MS) found 530.0847, calcd for  $C_{23}H_{25}BrN_5O_3S$  530.0861  $[M + H]^+$ . HPLC purity > 96%,  $rt = 10.5$  min.

(*E*)-6-(1-(2-carbamothioylhydrazono)ethyl)-1-(2,4-dichlorobenzyl)-*N*-(2-methoxyethyl)-4-oxo-1,4-dihydroquinolone-3-carboxamide, **19**. Brown powder. Yield = 65% (0.27 g). m.p.: 209–211 °C.  $^1H$ -NMR (300 MHz, DMSO- $d_6$ )  $\delta_H$  (ppm): 10.34 (s, 1H, CSNHN), 10.05 (s, 1H, CONH), 9.07 (s, 1H, Ar-H), 8.64 – 8.47 (m, 2H, Ar-H), 8.35 (s, 1H, NH), 8.03 (s, 1H, NH), 7.73 – 7.44 (m, 3H, Ar-H), 7.18 (s, 1H, Ar-H), 5.82 (s, 2H,  $-CH_2Ar$ ), 3.66 – 3.46 (m, 6H,  $2 \times -CH_2$ , overlap with H<sub>2</sub>O), 3.31 (s, 3H,  $-OCH_3$ ), 2.37 (s, 3H, CH<sub>3</sub>).  $^{13}C$  NMR (75 MHz, DMSO- $d_6$ )  $\delta$  179.5, 176.7, 164.1, 146.8, 144.6, 139.9, 138.3, 135.1, 134.6, 132.8, 131.9, 130.5, 129.6, 127.9, 127.4, 124.7, 118.8, 112.5, 71.3, 62.6, 58.5, 39.1, 14.7.  $m/z$  (ESI-MS): found 520.0857, calcd for  $C_{23}H_{24}Cl_2N_5O_3S$  520.0861  $[M + H]^+$ . HPLC purity > 96%,  $rt = 9.4$  min.

Methyl-(*E*)-1-(4-bromobenzyl)-6-(1-(2-carbamothioylhydrazono)ethyl)-4-oxo-1,4-dihydroquinolone-3-carboxylate, **20**. Off white powder. Yield = 60% (0.25 g). m.p.: 203–205 °C.  $^1H$ -NMR (300 MHz, DMSO- $d_6$ )  $\delta_H$  (ppm): 10.31 (s, 1H, CSNHN), 8.94 (s, 1H, Ar-H), 8.52 – 8.38 (m, 3H, Ar-H), 8.30 (s, 1H, NH), 7.99 (s, 1H, NH), 7.55 (d,  $J = 8.7$  Hz, 2H, Ar-H), 7.23 (d,  $J = 8.7$  Hz, 2H, Ar-H), 5.69 (s, 2H,  $-CH_2Ar$ ), 3.78 (s, 3H,  $-OCH_3$ ), 2.34 (s, 3H,  $-CH_3$ ).  $^{13}C$ -NMR (75 MHz, DMSO- $d_6$ )  $\delta_C$  (ppm): 179.5, 173.5, 164.9, 150.5, 146.4, 139.2, 135.9, 135.1,

132.3, 131.05, 129.6, 128.3, 124.7, 121.4, 118.8, 111.0, 55.0, 51.8, 14.7. m/z (ESI-MS) found 487.0437, calcd for  $C_{21}H_{20}BrN_4O_3S$  487.0439  $[M + H]^+$ . HPLC purity > 96%, rt = 8.5 min.

*Ethyl-(E)-6-(1-(2-carbamothioylhydrazono)ethyl)-1-(2,4-dichlorobenzyl)-4-oxo-1,4-dihydroquinolone-3-carboxylate*, **21**. Brown powder. Yield = 60% (0.23 g). m.p.: 211–213 °C.  $^1H$ -NMR (300 MHz, DMSO- $d_6$ )  $\delta_H$  (ppm): 10.35 (s, 1H, CSNHN), 8.92 (s, 1H, Ar-H), 8.58–8.41 (m, 2H, Ar-H), 8.33 (s, 1H, NH), 8.03 (s, 1H, NH), 7.75–7.38 (m, 3H, Ar-H), 7.17 (d,  $J = 9.0$  Hz, 1H, Ar-H), 5.72 (s, 2H,  $-CH_2Ar$ ), 4.24 (q,  $J = 6.7$  Hz, 2H,  $-OCH_2-$ ), 2.34 (s, 3H,  $CH_3$ ), 1.30 (t,  $J = 6.7$  Hz, 3H,  $-CH_3$ ).  $^{13}C$ -NMR (75 MHz, DMSO- $d_6$ )  $\delta_C$  (ppm): 179.5, 173.2, 164.9, 150.5, 146.4, 140.5, 136.4, 134.6, 133.7, 132.8, 131.9, 129.6, 128.7, 127.9, 126.9, 124.2, 118.4, 111.6, 60.4, 54.9, 15.5, 14.2. m/z (ESI-MS) found 491.0610, calcd for  $C_{22}H_{21}Cl_2N_4O_3S$  491.0615  $[M + H]^+$ . HPLC purity > 96%, rt = 9.4 min.

### 3.3. In Vitro Anti-Plasmodial Assay

The 3D7 strain of *Plasmodium falciparum* was routinely cultured in medium consisting of RPMI1640 containing 25 mM Hepes (Lonza), supplemented with 0.5% (w/v) Albumax II (ThermoScientific), 22 mM glucose, 0.65 mM hypoxanthine, 0.05 mg/mL gentamicin and 2–4% (v/v) human erythrocytes. Cultures were maintained at 37 °C under an atmosphere of 5%  $CO_2$ , 5%  $O_2$ , 90%  $N_2$ . To assess antiplasmodial activity, three-fold serial dilutions of test compounds in culture medium were added to parasite cultures (adjusted to 2% parasitaemia, 1% haematocrit) in 96-well plates and incubated for 48 h. Duplicate wells per compound concentration were used. Parasite lactate dehydrogenase (pLDH) enzyme activity in the individual wells was determined as previously described [35,36].

### 3.4. In Vitro Cytotoxicity Assay

As previously described [37], HeLa cells (Cellonex) seeded in 96-well plates were incubated with 20  $\mu M$  test compounds for 24 h and cell viability assessed using a resazurin fluorescence assay.

### 3.5. In Vitro Antimycobacterial Assay

The minimum inhibitory concentration (MIC) was determined using the standard broth microdilution method, where a 10 mL culture of *Mycobacterium tuberculosis* pMSP12::GFP [38], was grown to an optical density (OD<sub>600</sub>) of 0.6–0.7. The medium used was Middlebrook 7H9 supplemented with 0.03% casitone, 0.4% glucose, and 0.05% tyloxapol [39]. Cultures grown in the medium were diluted 1:500, prior to inoculation in the MIC assay. The compounds to be tested were reconstituted to a concentration of 10 mM in DMSO. Two-fold serial dilutions of the test compound were prepared across a 96-well micro titre plate, after which, 50  $\mu L$  of the diluted *Mtb* cultures was added to each well in the serial dilution. Assay controls used were a minimum growth control (Rifampicin at  $2 \times$  MIC), and a maximum growth control (5% DMSO). The micro titre plates were sealed in a secondary container and incubated at 37 °C with 5%  $CO_2$  and humidification. Relative fluorescence (excitation 485 nm; emission 520 nm) was measured using a plate reader (FLUOstar OPTIMA, BMG LABTECH), at day 7 and day 14. The raw fluorescence data were archived and analysed using the CDD Vault from Collaborative Drug Discovery, in which data were normalised to the minimum and maximum inhibition controls to generate a dose response curve (% inhibition), using the Levenberg-Marquardt damped least squares method, from which the MIC<sub>90</sub> was calculated (Burlingame, CA [www.collaboratedrug.com](http://www.collaboratedrug.com)). The lowest concentration of drug that inhibited growth of more than 90% of the bacterial population was considered the MIC<sub>90</sub>.

## 4. Conclusions

In this study, quinolone-thiosemicarbazones were obtained in high yields through simple and cost effective classical synthetic transformations without the use of specialised equipment and expensive catalysts. The compounds reported herein showed no growth inhibition of HeLa cells at a concentration of 20  $\mu M$  suggesting the general lack of cytotoxicity by this series. More importantly, this series

exhibited good activities against *P. falciparum*, and *M. tuberculosis*, the pathogens responsible for malaria, and tuberculosis, respectively. Overall, the presented data suggest that quinolone-thiosemicarbazones are a compound class worth further exploitation in search of cheap molecules with dual activities against the aforementioned diseases-causing microorganisms.

**Supplementary Materials:** The following are available online (<sup>1</sup>H and <sup>13</sup>C NMR spectra, and HRMS spectra of compounds 11–21).

**Author Contributions:** R.M.B. and S.D.K. conceptualized target compounds. R.M.B. executed the synthesis and compiled the paper. R.S., A.J. and D.F.W. coordinated and performed the anti-mycobacterial assays. H.C.H. and D.L. coordinated and performed the anti-plasmodial and cytotoxicity assays. S.D.K. coordinated the investigation.

**Funding:** The authors acknowledge the financial support by the National Research Foundation (SDK, Grant number 107270), Rhodes University for Postdoctoral funding (RMB) and Rhodes University Sandisa Imbewu (SDK and HCH) towards this research. The antiplasmodial bioassay component of the project was funded by the South African Medical Research Council (MRC) with funds from National Treasury under its Economic Competitiveness and Support Package. All TB screening work was conducted in the MMRU (UCT) with the support of SAMRC through the Strategic Health Innovation Partnerships (SHIP) initiative (DFW). Our great appreciation to Christian Nkanga, Department of Chemistry, Rhodes University for HPLC purity data as well as Stellenbosch University Central for Analytical Facility (CAF) for mass spectrometric analysis.

**Conflicts of Interest:** The authors declare no conflict of interest.

## References

1. Delogu, G.; Sali, M.; Fadda, G. The biology of *Mycobacterium tuberculosis* infection. *Mediterr. J. Hematol. Infect. Dis.* **2013**, *5*, e2013070. [[CrossRef](#)]
2. Bañuls, A.L.; Sanou, A.; Anh, N.T.; Godreuil, S. *Mycobacterium tuberculosis*: Ecology and evolution of a human bacterium. *J. Med. Microbiol.* **2015**, *64*, 1261–1269. [[CrossRef](#)]
3. Ahmad, S. Pathogenesis, immunology, and diagnosis of latent *Mycobacterium tuberculosis* infection. *Clin. Dev. Immunol.* **2011**, *2011*, 1–17. [[CrossRef](#)] [[PubMed](#)]
4. Lin, P.L.; Flynn, J.-A.L. The end of the binary era: Revisiting the spectrum of tuberculosis. *J. Immunol.* **2018**, *201*, 2541–2548. [[CrossRef](#)]
5. Ai, J.-W.; Ruan, Q.-L.; Liu, Q.-H.; Zhang, W.-H. Updates on the risk factors for latent tuberculosis reactivation and their managements. *Emerg. Microbes Infect.* **2016**, *5*, e10. [[CrossRef](#)] [[PubMed](#)]
6. Dargie, B.; Tesfaye, G.; Worku, A. Prevalence and associated factors of undernutrition among adult tuberculosis patients in some selected public health facilities of Addis Ababa, Ethiopia: A cross-sectional study. *BMC Nutr.* **2016**, *2*, 7. [[CrossRef](#)]
7. Cudahy, P.; Sheno, S. Diagnostics for pulmonary tuberculosis. *Postgrad. Med. J.* **2016**, *92*, 187–193. [[CrossRef](#)]
8. Churchyard, G.; Kim, P.; Shah, N.; Rustomjee, R.; Gandhi, N.; Mathema, B.; Dowdy, D.; Kasmar, A.; Cardenas, V. What we know about tuberculosis transmission: An overview. *J. Infect. Dis.* **2017**, *216*, S629–S635. [[CrossRef](#)] [[PubMed](#)]
9. WHO. *Global Tuberculosis Report 2018*; WHO: Geneva, Switzerland, 2018; ISBN 978-92-4-156564-6.
10. Lohrasbi, V.; Talebi, M.; Bialvaei, A.; Fattorini, L.; Drancourt, M.; Heidary, M.; Darban-Sarokhalil, D. Trends in the discovery of new drugs for *Mycobacterium tuberculosis* therapy with a glance at resistance. *Tuberculosis* **2018**, *109*, 17–27. [[CrossRef](#)]
11. Auld, S.C.; Shah, N.S.; Mathema, B.; Brown, T.S.; Ismail, N.; Omar, S.V.; Brust, J.C.; Nelson, K.; Allana, S.; Campbell, A.; et al. XDR tuberculosis in South Africa: Genomic evidence supporting transmission in communities. *Eur. Respir. J.* **2018**, *52*, 1800246. [[CrossRef](#)] [[PubMed](#)]
12. WHO. *World Malaria Report 2017*; WHO: Geneva, Switzerland, 2017; pp. 32–43.
13. WHO. *World Malaria Report 2015*; WHO: Geneva, Switzerland, 2015.
14. Gomes, A.P.; Vitorino, R.R.; Costa, A.; de Mendonça, E.; Oliveira, M.; Siqueira-Batista, R. Severe *Plasmodium falciparum* malaria. *Rev. Bras. Ter. Intensiva* **2011**, *23*, 358–369. [[CrossRef](#)] [[PubMed](#)]
15. Olliaro, P. Mortality associated with severe *Plasmodium falciparum* malaria increases with age. *Clin. Infect. Dis.* **2008**, *47*, 158–160. [[CrossRef](#)]
16. Snow, R.S. Global malaria eradication and the importance of *Plasmodium falciparum* epidemiology in Africa. *BMC Med.* **2015**, *13*, 23. [[CrossRef](#)] [[PubMed](#)]

17. Salmanzadeh, S.; Foroutan-Rad, M.; Khademvatan, S.; Moogahi, S.; Bigdeli, S. Significant decline of malaria incidence in southwest of Iran (2001–2014). *J. Trop. Med.* **2015**, *2015*, 1–6. [[CrossRef](#)] [[PubMed](#)]
18. Hay, S.I.; Guerra, C.A.; Tatem, A.J.; Atkinson, P.M.; Snow, R.W. Urbanization, malaria transmission and disease burden in Africa. *Nat. Rev. Microbiol.* **2005**, *3*, 81–90. [[CrossRef](#)] [[PubMed](#)]
19. Mbengue, A.; Bhattacharjee, S.; Pandharkar, T.; Liu, H.; Estiu, G.; Stahelin, R.; Rizk, S.; Njimoh, D.; Ryan, Y.; Chotivanich, K.; et al. A molecular mechanism of artemisinin resistance in *Plasmodium falciparum* malaria. *Nature* **2015**, *520*, 683–687. [[CrossRef](#)]
20. Mita, T.; Tanabe, K. Evolution of *Plasmodium falciparum* drug resistance: Implications for the development and containment of artemisinin resistance. *Jpn. J. Infect. Dis.* **2012**, *65*, 465–475. [[CrossRef](#)] [[PubMed](#)]
21. Pousibet-Puerto, J.; Salas-Coronas, J.; Sánchez-Crespo, A.; Molina-Arrebola, A.; Soriano-Pérez, M.; Giménez-López, M.; Vázquez-Villegas, J.; Cabezas-Fernández, M. Impact of using artemisinin-based combination therapy (ACT) in the treatment of uncomplicated malaria from *Plasmodium falciparum* in a non-endemic zone. *Malar. J.* **2016**, *15*, 339. [[CrossRef](#)]
22. Pasvol, G. The treatment of complicated and severe malaria. *Br. Med. Bull.* **2005**, *75–76*, 29–47. [[CrossRef](#)]
23. Cui, L.; Mharakurwa, S.; Ndiaye, D.; Rathod, P.; Rosenthal, P. Antimalarial drug resistance: Literature review and activities and findings of the ICEMR network. *Am. J. Trop. Med. Hyg.* **2015**, *93*, 57–68. [[CrossRef](#)]
24. Marriner, G.A.; Nayyar, A.; Uh, E.; Wong, S.; Mukherjee, T.; Via, L.; Carroll, M.; Edwards, R.; Gruber, T.; Choi, I.; et al. The medicinal chemistry of tuberculosis chemotherapy. *Top. Med. Chem.* **2011**, *7*, 47–124.
25. Li, X.-X.; Zhou, X.-N. Co-infection of tuberculosis and parasitic diseases in humans: A systematic review. *Parasit. Vectors* **2013**, *6*, 79. [[CrossRef](#)]
26. Murphy, M.E.; Singh, K.P.; Laurenzi, M.; Brown, M.; Gillespie, S.H. Managing malaria in tuberculosis patients on fluoroquinolone-containing regimens: Assessing the risk of QT prolongation. *Int. J. Tuberc. Lung Dis.* **2012**, *16*, 144–149. [[CrossRef](#)]
27. Grzegorzewicz, A.E.; Korduláková, J.; Jones, V.; Born, S.; Belardinelli, J.; Vaquié, A.; Gundi, V.; Madacki, J.; Slama, N.; Laval, F.; et al. A Common mechanism of inhibition of the *Mycobacterium tuberculosis* mycolic acid biosynthetic pathway by Isoxyl and Thiacetazone. *J. Biol. Chem.* **2012**, *287*, 38434–38441. [[CrossRef](#)] [[PubMed](#)]
28. Greenbaum, D.; Mackey, Z.; Hansell, E.; Doyle, P.; Gut, J.; Caffrey, C.R.; Lehman, J.; Rosenthal, P.J.; McKerrow, J.H.; Chibale, K. Synthesis and structure activity relationships of parasitocidal thiosemicarbazone cysteine protease inhibitors against *Plasmodium falciparum*, *Trypanosoma brucei* and *Trypanosoma cruzi*. *J. Med. Chem.* **2004**, *47*, 3212–3219. [[CrossRef](#)]
29. Akhtar, R.; Yousaf, M.; Naqvi, S.; Irfan, M.; Zahoor, A.; Hussain, A.; Chatha, S. Synthesis of ciprofloxacin-based compounds: A review. *Syn. Commun.* **2016**, *46*, 1849–1879. [[CrossRef](#)]
30. Dixit, S.; Mishra, N.; Sharma, M.; Singh, S.; Agarwal, A.; Awasthi, S.; Bhasin, V. Synthesis and in vitro antiplasmodial activities of fluoroquinolone analogs. *Eur. J. Med. Chem.* **2012**, *51*, 52–59. [[CrossRef](#)] [[PubMed](#)]
31. Beteck, R.M.; Seldon, R.; Jordaan, A.; Warner, D.F.; Hoppe, H.C.; Laming, D.; Legoabe, L.J.; Khanye, S.D. Quinolone-isoniazid hybrids: Synthesis and preliminary in vitro cytotoxicity and anti-tuberculosis evaluation. *Medchemcomm* **2019**, *10*, 326–331. [[CrossRef](#)]
32. Neelapapu, R.; Maignan, J.; Lichorowic, C.; Monastyrskyi, A.; Mutka, T.; LaCrue, A.; Blake, L.; Casandra, D.; Mashkouri, S.; Burrows, J.; et al. Design and synthesis of orally bioavailable piperazine substituted 4(1H)-quinolones with potent antimalarial activity: Structure-activity and structure-property relationship studies. *J. Med. Chem.* **2018**, *61*, 1450–1473. [[CrossRef](#)]
33. Venkatachalam, T.K.; Pierens, G.K.; Reutens, D.C. Synthesis, NMR structural characterization and molecular modeling of substituted thiosemicarbazones and semicarbazones using DFT calculations to prove the syn/anti isomer formation. *Magn. Reson. Chem.* **2014**, *52*, 98–105. [[CrossRef](#)]
34. Beteck, R.M.; Isaacs, M.; Hoppe, H.C.; Khanye, S.D. Synthesis, in vitro cytotoxicity and trypanocidal evaluation of novel 1,3,6-substituted non-fluoroquinolones. *S. Afr. J. Chem.* **2018**, *71*, 188–195. [[CrossRef](#)]
35. Gumbo, M.; Beteck, R.M.; Mandizvo, T.; Seldon, R.; Warner, D.F.; Hoppe, H.C.; Isaacs, M.; Laming, D.; Tam, C.C.; Cheng, L.W.; et al. Cinnamoyl-oxaborole amides: Synthesis and their in vitro biological activity. *Molecules* **2018**, *23*, 2038. [[CrossRef](#)] [[PubMed](#)]

36. Mbaba, M.; Mabhula, A.N.; Boelb, N.; Edkinsb, A.L.; Isaacs, M.; Hoppe, H.C.; Khanye, S.D. Ferrocenyl and organic novobiocin derivatives: Synthesis and their in vitro biological activity. *J. Inorg. Biochem.* **2017**, *172*, 88–93. [[CrossRef](#)] [[PubMed](#)]
37. Oderinlo, O.O.; Tukulula, M.; Isaacs, M.; Hoppe, H.C.; Taylor, D.; Smith, V.J.; Khanye, S.D. New thiazolidine-2,4-dione derivatives combined with organometallic ferrocene: Synthesis, structure and antiparasitic activity. *Appl. Organomet. Chem.* **2018**, *32*, e4385. [[CrossRef](#)]
38. Abrahams, K.A.; Cox, J.G.; Spivey, V.L.; Loman, N.J.; Pallen, M.J.; Constantinidou, C.; Fernández, R.; Alemparte, C.; Remuñuínán, M.J.; Barros, D.; et al. Identification of novel imidazo[1,2-a]pyridine inhibitors targeting M. tuberculosis QcrB. *PLoS ONE* **2012**, *7*, e52951. [[CrossRef](#)] [[PubMed](#)]
39. De Voss, J.J.; Rutter, K.; Schroeder, B.G.; Su, H.; Zhu, Y.; Barry, C.E., III. The salicylate-derived mycobactin siderophores of *Mycobacterium tuberculosis* are essential for growth in macrophages. *PNAS* **2000**, *97*, 1252–1257. [[CrossRef](#)] [[PubMed](#)]

**Sample Availability:** Samples of all the compounds are available from the authors.



© 2019 by the authors. Licensee MDPI, Basel, Switzerland. This article is an open access article distributed under the terms and conditions of the Creative Commons Attribution (CC BY) license (<http://creativecommons.org/licenses/by/4.0/>).